3

A biologically founded design and control of a humanoid biped

Giuseppina C. Gini, Michele Folgheraiter, Umberto Scarfogliero
and Federico Moro
DEI, Politecnico di Milano
Italy

1. Introduction

During the last decade many advancements in the fields of industrial and service robotics have produced robots that are well integrated inside the industry; they can operate faster and with higher precision in comparison to human beings. Nevertheless if we take a look at the kinematic structure of these systems, it is clear that the actual machines are limited in the mobility and in the number of tasks that they can perform.
This is more evident if we intend to apply those robots in an unstructured environment like home. First at all the robot should be able to move around avoiding obstacles, climbing stairs, opening doors. These movements should also be performed with a certain level of compliance for the safety of the human beings that are in the environment. Secondly, the robots should be able to use tools and other machines designed for human use, and based of the human manipulation and kinematic abilities.
A possible solution for mobility, that is well applied in mobile robotics, is the choice of a wheeled traction system. This usually is a simple manner to move on flat floors, and is efficient from the energetic point of view (during the movement the center of mass acts on a straight line). However it presents important limitations, for example it is not possible for such a robot to overcome obstacles bigger than the wheels dimensions.
Those limitations can be overcome if the robot is equipped with legs, that normally act by increasing the robot's DOF(Degrees of Freedom). Many studies were conducted on legged robot in order to improve the efficiency and stability during walking.
A pioneering contribution was done (Takanishi et al, 2004) at the laboratories of Waseda University (Tokyo). Several other modern robots are designed to walk and behave like humans (Hashimoto et al, 2002)(**3**) but until now the efficiency of the human gait is still far from being reached. In this sense, the work of McGeer (McGeer, 1990) can be considered exemplar. His passive dynamic walker made a stable gait without close position control, considering the walking motion as a natural oscillation of a double pendulum; and this is actually how humans seem to walk (Gottlieb et al, 1996) (Kiriazov, 1991)**.** His results inspired many other works, such as the stability analysis (Garcia et al, 1998) and the physical implementation (Wisse et al, 2001) (Kuo, 1999)(Collins et al, 2001) of several prototypes.

In this paper we present LARP (*Light Adaptive-Reactive biPed*), our humanoid legged system, with the aim to explain how the mechanical design makes the robot able to adapt to the real operating environment. Our aim was to create a system that could represent a good model of human lower limbs, in order to understand how the natural walking motion is achieved and how it can be implemented in a humanoid robot. For this reason, we adopted anthropomorphic feet, knees and a mass-distribution similar to the human limbs.
According to (McGeer, 1990)} we designed an actuation system that can take advantage of the natural dynamics of the link. In addition, studying the results we got from our controller we found several similarities with the assumptions of the Equilibrium Point Theory. This is a widely debated theory, formulated in 1965 by A. Feldman (Asatryan, 1965) (Asatryan and Feldman, 1966 a) (Asatryan and Feldman, 1966 b) and still in evolution. This theory proposes that the segmental reflexes, together with the muscle-skeletal system, behave like a spring. Movement is achieved just by moving the equilibrium position of that spring (Latash and Gottlieb, 1991) (McIntyre and Bizzi, 1993) (Gottlieb et al, 1989) and this is actually how our actuator, provided with visco-elastic elements (Scarfogliero et al, 2004 a) performs the movement.
In the following Sections we concentrate our attention on the robot design and architecture, with particular emphasis on the knee, which presents several similarities to the human articulation, and the foot, developed with two passive degrees of freedom. Then we illustrate the spring-damper actuators and joint controller. We present the robot simulator and the results obtained in computing the energy consumption of LARP. Finally we shortly describe the controller for the gait. The last section outlines the conclusions we can draw from our work and proposes future developments.

2. The mechanical architecture

The LARP project started in 2003 in the Artificial Intelligence and Robotics Lab of DEI, at Politecnico di Milano. It soon provided a 3D model developed in ADAMS and a prototype, as shown in Figure 1. LARP has twelve active degrees of freedom plus two passive degrees for each leg; it is ninety cm tall and weights less than five kg. It is entirely made by pieces cut out from a polycarbonate sheet with the laser cutting technology; this material has a good strength-weigh ratio, and can be widely deformed before breaking.

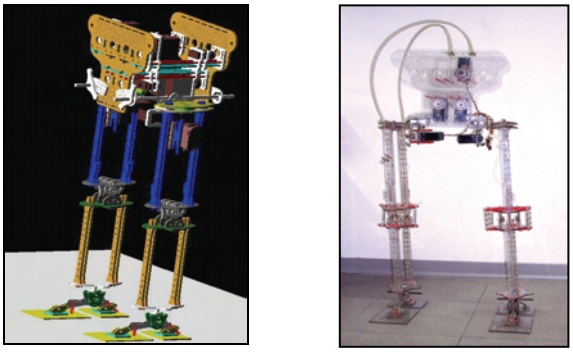

Fig. 1. The LARP robot. (a) the ADAMS model, (b) the mechanical prototype with some actuators installed.

Figure 2 shows the organization of the twelve degrees of freedom in the robot. The range of motion of each joint is similar to that of humans during normal walking.

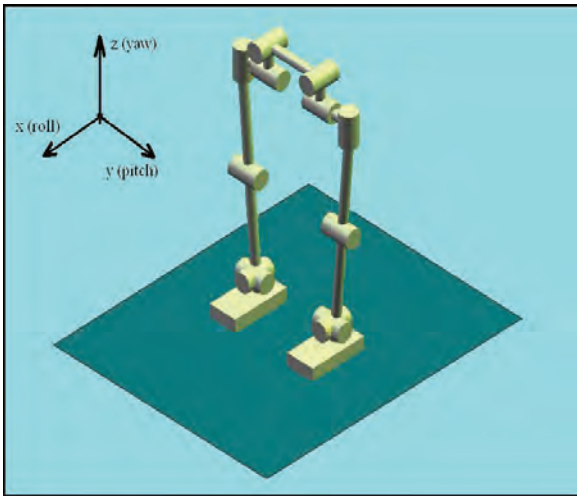

Fig. 2. The organization of the twelve degrees of freedom in LARP.

Each foot has two passive degrees of freedom to ensure a reliable base during the whole stance phase. Joint torques are provided by servo motors located in the upper part of the robot. The transmission is performed by a simple system of cables and levers. The servo motors are equipped with a spring and a damper to permit the control of joint stiffness.
The mechanical design of LARP focused on role and function of knee and foot.
Regarding the knee functions, the most obvious is lifting the shank for the foot clearance. In practice, if that was the only purpose of that joint, an hip articulation could make the job. Using stiff legs could actually simplify the motion and the robot structure (examples of this kind of robots go back to the simple Fallis's toy (Fallis, 1888) to the various 3D biped robots of MIT LegLab. In practice, however, the knee has several important functions in the walking dynamics, that suggest the introduction of the knee articulation.
Also the foot has important consequences on the dynamics of the step, and deserves more investigations. Usually legged robots have simple flat feet, or no feet al all; the foot in biped instead is flexible and accounts for important roles.

3. The design of an anthropomorphic knee

3.1 The importance of the knee in bipeds

It is well known that it is possible to walk with stiff legs, however it is also known that knee articulation is fundamental for the gait stability and energy efficiency. The story of artificial bipeds is plenty of simple prototypes walking without anthropomorphic knees. The importance of knee actuation became more clear when considering the gait efficiency. In 1990 Tad McGeer published "Passive Dynamic Walking" (PDW), where he demonstrated how it is possible to exploit the mass distribution of the robot to make it walk on a shallow

slope without actuation (McGeer, 1990). The prototype was exploiting the gravity force to swing the leg forward, exactly as a double pendulum would do. The only power needed was the one necessary to shorten the leg in order to create foot clearance during the swinging motion. Today, several passive dynamic walkers have been developed, but in order to have a fully-passive walker, it became necessary to add knee joints (McGeer, 1990)(Wisse et al, 2002). As a matter of facts, this joint empowers the swinging motion due to gravity, and with the right mass distribution, it is possible to perform a fully-passive pace.

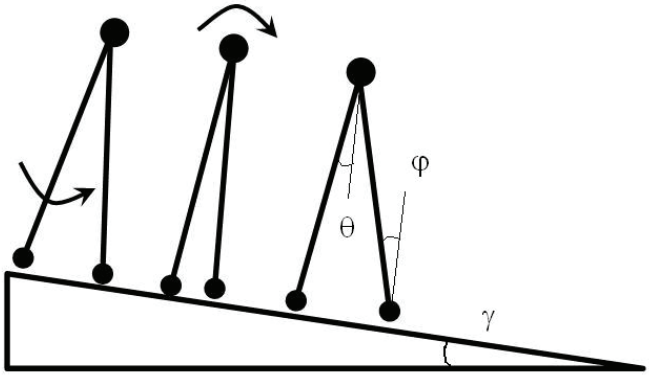

Fig. 3. With the right mass distribution of the robot it is possible to make it walk on a shallow slope without actuation, as demonstrated by Passive Dynamic Walkers

Apart from PDW, the knee is fundamental to ensure energetic efficiency. Let's consider a robot with straight legs. In this case the foot clearance would have to be created by an additional pelvic tilt. This means a reduced step length and a bigger energy consumption, as the pelvis is the heaviest part of the body while knee stretching just lift the foot. This has a big influence on walking efficiency (Koopman et al, 2001) Another effect of straight legs would be that, during the step, the double support time is decreased, on behalf of the single support time. As the former is the most stable position during the step, the straight leg walking is more critical from the stability point of view. So knee-walking needs less energy to ensure gait stability.

The knee is important also during the stance phase, while the supporting leg remains straight. In this case, while the swinging leg moves forward, the knee of the stance leg has to counteract the inertial load generated by gait motion, as shown in Figure 4. In this case the knee can be exploited to store energy, acting as a spring. This energy can be used to pull the hip forward, increasing the step length and the foot clearance. Using a force control to actuate the knee, as we discussed in (Scarfogliero et al, 2004 b) it is possible to store energy, exploiting in this way the natural dynamics of the walking motion. The same happens in humans: during the stance phase, the knee bends a bit, storing energy as a spring would do. This energy is then released to empower the hip forward motion, with a relevant increase in the step length and foot clearance. The result is that the gait performs, with the same energy

consumption, a more stable walk. This behavior was also underlined by simulations on a PDW, the robot Mike, of the Delft University of Technology (Wisse et al, 2002).

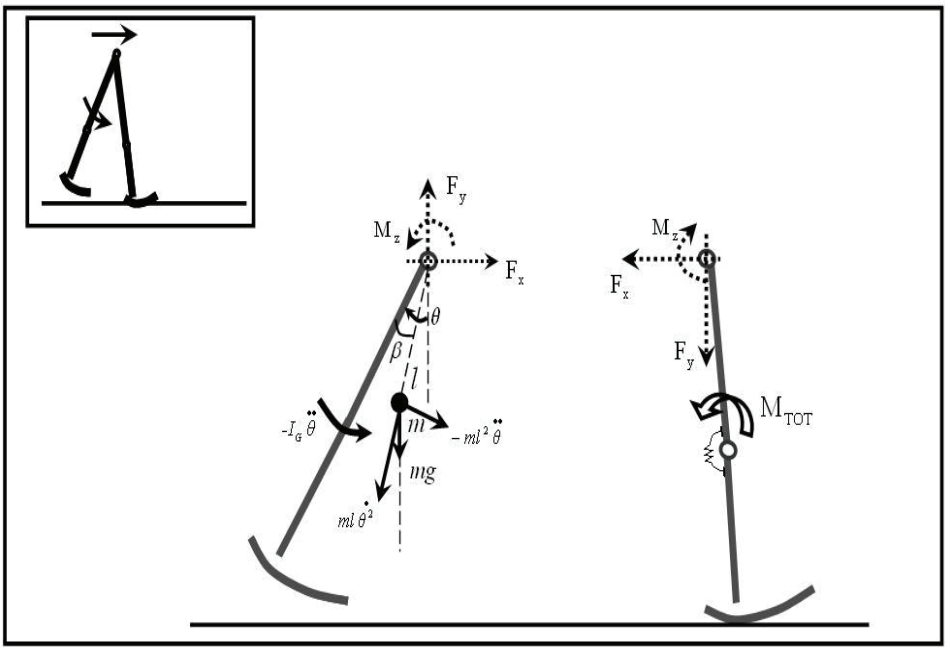

Fig. 4. During walking, the knee of the stance leg has to counteract the inertial loads due to the swinging motion.

3.2 The design of the knee joint

Regarding the knee structure the most obvious and more adopted solution in robotics is a simple pin joint. Usually the motor is applied directly to the joint, but there are also some examples where, for mass-distribution reasons, the motor is placed in the upper part of the robot (Pratt et al, 2001).

Looking at the prosthesis field, we find a completely different approach. Here the knee reveals its crucial importance, not only related to the prosthetic issues, but also for the walking motion. Passive prosthesis have to perform the knee bending using inertial torque generated by the forward acceleration of the thigh, in a similar manner as in passive dynamic walking. In addition, for obvious safety reasons, during the stance phase the knee has to be locked.

Today, prosthetic knees are build using multi-axial mechanisms. The characteristic of these mechanisms is that during the motion, the center of rotation *cr* is not fixed, as in a pin joint, but moves along a trajectory that depends on the mechanism structure. As the stability of the knee during the stance phase strongly depends on the position of *cr*, varying the mechanism proportions, it is possible to have different *cr* trajectories with different stability properties, as illustrated in Figure 5.

Fig. 5. Scheme of a four-axial mechanism for a prosthetic knee. The dotted line represents the path followed by the centre of rotation cr. The big dot represents the cr when the knee is extended. Placing this point more backward, results in a more stable stance phase

For LARP we designed a special joint based on the human articulation. If we sketch the human knee from an engineering point of view, we would define it as an hybrid juncture, similar to a compliant joint but with rolling surfaces. This structure is very close to the compliant rolling-contact joint designed by (Jeanneau et al, 2004) and illustrated in Fig. 6.

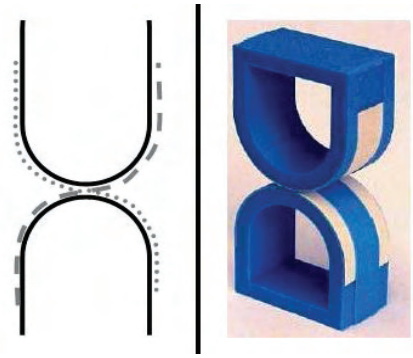

Fig. 6. The compliant rolling-contact joint designed by Herder. Reprinted with permission from J. Herder (Jeanneau et al, 2004)

Our joint is composed by two circular surfaces rolling on each other. Flexible bands constrain the joint, leaving only one degree of freedom, i.e. the rotation along the joint axis. During the motion, the tendons wrap on a surface or on the other, letting the joint rotate without scratch. This significantly reduces friction.
Critical in this kind of joint are the torsional stiffness and the rigidity against external forces. This issue is fundamental for the biped robots, where the knee is subject to high torsional and flexional disturbances. To solve this aspect, we strengthened the joint, designing the articulation shown in Fig. 7. Instead of flexible bands, we used three Coramide strings that can all be independently fastened. This makes the articulation more firm as well as allows a

fine joint calibration. In addition, we added two springs, which increase the contact force between the circular surfaces. Connecting the spring ends at the center of curvature of the two profiles, results in a constant spring-length - equal to two times the radius of the profile. In this case no torque interferes with the joint rotation. Anyhow, it is possible to arrange the springs in a way that they force the joint to rotate to a particular equilibrium position.

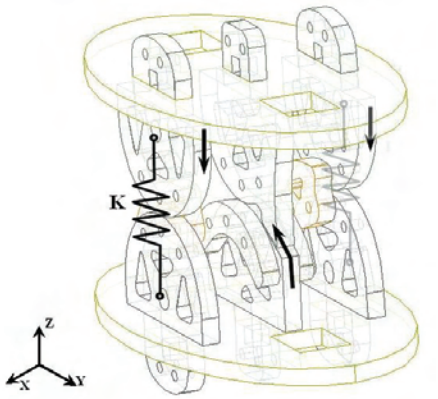

Fig. 7. The knee joint designed for our robot. The arrows show the way the tendons are wrapped.

In the knee we arranged the springs as shown in Fig. 8, so that during the rotation, the spring length has a maximum for a given θ (where θ is the angle that the shank forms with the vertical). In Fig. 8, γ represents the angle between the shank axis and the force direction. When γ is zero, the springs torque is zero too. This permits to find one equilibrium position, in particular, an instable equilibrium position, as the spring is at its maximum extension. Attaching the spring forward, with ψ <0, we can both help knee bending during leg swinging and knee stretching at the end of the step.

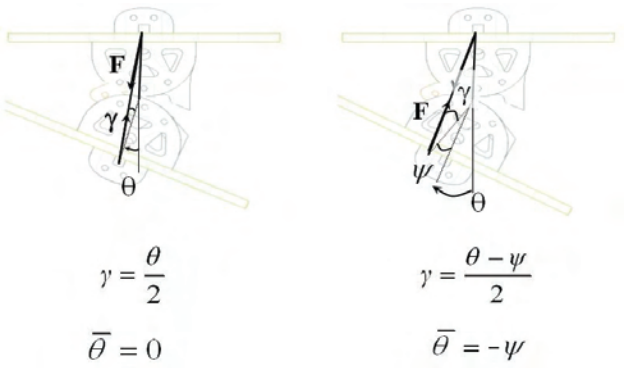

Fig. 8. We can exploit the action of the springs to impose a suited torque on the joint. In particular, it is possible to generate the two positions of instable equilibrium to favour knee bending and knee stretching.

Adopting this kind of joint for the knee articulation has several advantages with respect to a pin joint. The first consideration is about energy efficiency. A reduced friction at the knee not only reduces knee actuation, but can influence the whole gait. As pointed out in the previous paragraph, using elastic actuators or even a passive knee, the leg can be bent exploiting inertial forces due to hip actuation. In this sense, efficient knee joint is fundamental not to demand higher hip torque. Another aspect that strongly characterizes this compliant joint is that the center of rotation *cr* is not fixed, as in a pin joint, but moves upward and backward during the rotation, as illustrated in Fig. 9.

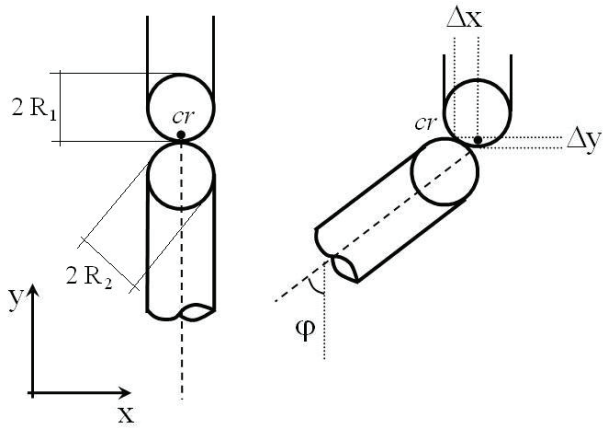

Fig. 9. When the leg is bending, the center of rotation moves upward and backward, according to the ratio between R1 and R2, the radius of the rolling surfaces.

This motion increases the foot clearance necessary to swing the leg, and the shank active rotation can thus be reduced. The effect is not only on energy consumption - i.e. the knee could be passive in some robots - but also on the gait stability. Actually the inertial load of knee-bending and knee-stretching is one of the most important in the dynamics of walking. This is also the reason why the foot must be designed as light as possible, as described in the next paragraph.

Regarding the radius of curvature of the two surfaces, we can look for an optimal design to maximize the foot clearance during the rotation. We can consider that if one contact surface (for example the upper one) has radius infinite or zero, the upward translation is null during the rotation. This means that there must be a finite rate value of the two radius that maximizes the upward motion. Considering that the two surfaces are in contact without slipping, the upward motion Δy, as in Fig. 10, is so computed:

$$\alpha R1 = \theta R2 \tag{1}$$

$$\Delta y = R1(1 - \cos(\alpha) = R1(1 - \cos(\theta\, R2/R1) \tag{2}$$

If R1 is fixed and we vary R2, the maximum can be found quite straightforward given θs:

$$R2 = (\pi / \theta s)R1 \quad (3)$$

θs is the angle of the bent knee in the instant the foot is closer to the ground.
According to this simple analysis, the radius R2 should be longer than R1; the bigger the ratio between the two radius, the smaller the shank rotation, till having a flat surface rolling on the upper one.

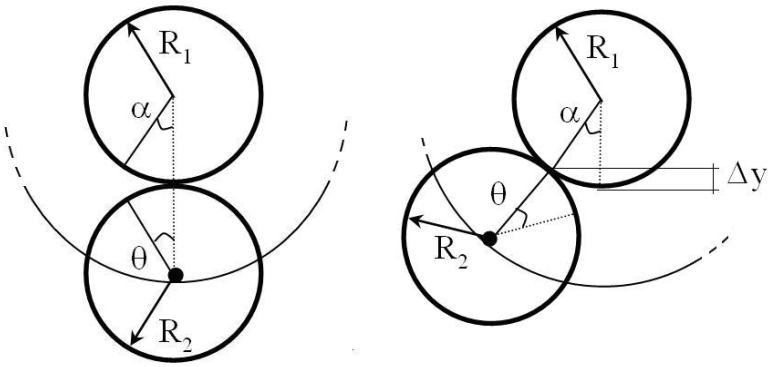

Fig. 10. The upward movement can be expressed as a function of R1, R2, and θ due to the constrain of rolling without slipping.

4. The role of the foot

4.1 The importance of foot in stability and efficiency of walking

The foot is probably the most challenging part for a biped robot to be anthropomorphic. Not only from the sensory point of view, but for the unique combination of mobility and lightness.
First of all, the foot inertia must be negligible with respect to the leg inertia. There are several evidences for this. One reason is the energy efficiency. To understand that, try to run or kick wearing heavy boots. During the swing-phase, the torque needed to move the leg forward is mainly due to inertial loads, that highly depend on the foot weight. In addition, these loads would act on the hip and the stance leg; their impact on the stability is more critical when the ratio body weight/foot weight is low.
But the foot does not only affect the dynamic balance. It is fundamental for stability to keep the center of mass as high as possible. At the beginning of the stance phase, the biped robot can be considered as an inverted pendulum, both in the fore-aft plane and in the frontal plane. Placing the center of mass higher increases the inertia of the pendulum respect to the hinge. It is well known that this implies slower changes respect to the initial position and thus a wider stability respect to external disturbances (Sardain, 1999). As already pointed out about the knee, stability and energy efficiency are strictly related. A more stable gait requires less motor action to counteract disturbances (Maloiy et al, 1986).
Another aspect that characterizes the human foot is its mobility and elasticity. (Ker et al. 1987) found that the foot behaves like an elastic body, returning about 78% of the energy in its elastic recoil. During running, the arc of the foot stores and returns 17% of the energy the

body loses and regains at each footfall, while till the 35% of this energy is stored and returned by Achilles tendon.
The foot mobility of course has a big influence on the whole kinematics and dynamics of the motion, especially on the ankle. In particular, during the stance phase, the contact point moves from the heel to the toe, and the foot is rotated before the toe-off. The position of the contact force plays a very important role in determining the joint torques, thus the energy consumption. As in normal walking the ground reaction is much higher than inertial forces, in first approximation, we can consider only this force acting on the stance leg (Vaughan, 1996). From this point of view, the bigger the arm between the joint and the contact force, the bigger would be the torque needed. In order to minimize energy consumption, while walking we naturally pose the leg joints close to the line of action of the contact force (Saunders et al, 1953) (Alexander, 1992). For this reason it is important to have a foot that let adapt the position of the ankle, and thus the other joints, without losing grip.
This aspect is particularly relevant at toe-off, when only a small region of the foot is in contact. Also here the mobility and elasticity of the foot plays a very important role (Doneland et al, 2002) (Kuo, 1998).
Fig. 11 shows a simple biped model at hell-strike: the rear leg is in the stance phase, and the fore leg is about at foot-fall. The energy loss at the impact depends on the vertical velocity of the center of mass *cm*. The ideal situation is when the *cm* velocity is parallel to the ground, and the legs simulate the wheel (McGeer, 1990). In normal walking, without toe-off the motion of the *cm* is rotational along the contact point of the stance leg. This means that at foot fall there is a component of *cm* vertical velocity that causes impact loss. Using toe-off, this component can be significantly reduced, resulting in a more efficient and smooth gait. (Kuo, 1998) figured out that providing all the energy necessary for walking by the toe-off muscle instead of the hip reduces the energy cost by a factor of 4.

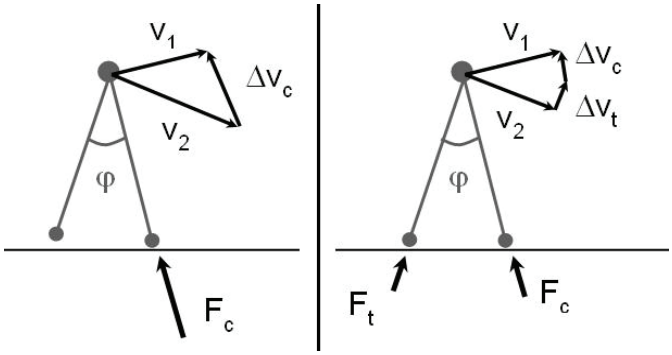

Fig. 11. Consider v1 and v2 as the velocities of the *cm*, respectively before and after heel-strike, while Fc and Ft are the ground reaction forces. With toe off (on the right) the *cm* vertical velocity is reduced, and the gait is smoother and more efficient.

4.2 The anthropomorphic foot

Nowadays, almost all the biped robots adopt a flat foot, with relatively heavy dampers to smooth the heel-strike; a noticeable exception is the design of toe joints proposed in (Sellaouti et al, 2006). The mobility of human foot is very difficult to reproduce, also because,

for walking stability, it is fundamental to keep the foot light. In the previous paragraph, we underlined that the key issues for the foot design are:

- The possibility to change ankle position without losing grip. This is a key issue for energy efficiency (Alexander, 1992)
- A good elasticity to store and release part of the energy lost at footfall. Also a good damping is required to smooth the impact occurring at every step
- The capacity to adapt to different ground situations without losing grip in different step phases, as at toe-off

Using a flat foot implies that the ankle position is fixed during the whole stance phase and, at toe-off, the contact is reduced to the foot edge as in Fig. 12. On the other hand, a flat foot is probably the simplest design that can be conceived, and ensures a big base on which to lean during the stance phase.

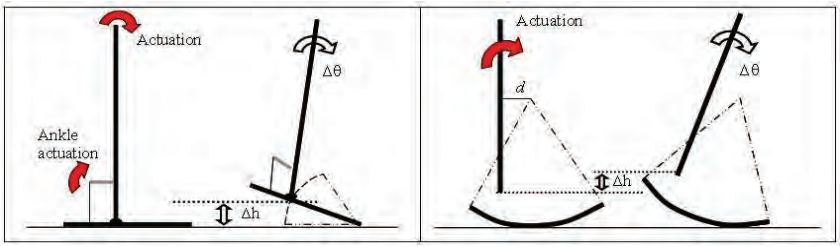

Fig. 12. A flat foot compared to a circular foot

Another type of simple foot profile, adopted mainly on passive dynamic walkers, is the round foot. The advantage of this kind of foot is that the ankle joint is moved forward during the rotation, minimizing in this way the torque needed at toe-off. The drawback of the round profile is that the contact surface is reduced to a thin area. That is way this kind of foot is mainly adopted on 2-D bipeds.

Thus, our goal was to develop a foot with the right trade-off between mobility and stability, keeping at the same time the structure as light as possible. So we adopted performing materials, mainly polycarbonate and carbon. Then, we designed the human-foot structure with a two-dof device, shown in Fig. 13. The foot has one passive degree of freedom that represent the heel, an arc, and another passive dof for the toe. In addition, we inserted an artificial Achilles tendon between the heel and the arc.

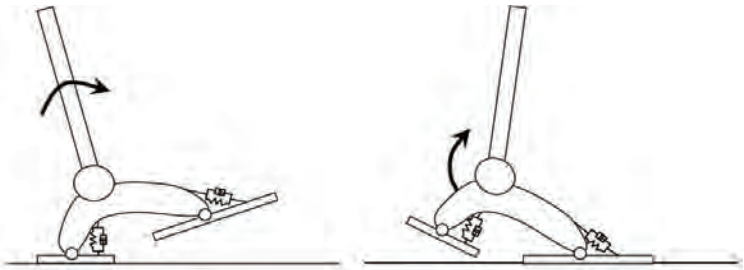

Fig. 13. The foot of LARP, developed to mimic the human one. It has two passive degrees of freedom, with a spring-damper system to smooth the heel-strike.

The articulations in the foot play an important role in determining the gait kinematics and dynamics. As shown in Fig. 13, at heel-strike and at toe-off, the ankle position is not constrained in one fixed position. This gives the ankle an addition degree of freedom, which makes it possible to minimize energy consumption as stated above.
Generally speaking, during the stance phase the contact position moves from the heel to the toe. With our foot, the center of rotation follows the same motion. This means that the lever arm of the ground reaction force is already reduced respect to a flat foot, where the ankle and the center of rotation are constrained in the same fixed point. Moreover, the foot keeps a firm base to lean even at toe-off, when the ankle is moved forward and upward for knee-bending. In this way the double support time - the time when both feet lean on the ground - can be increased, resulting in a more stable walk.
For simplicity, the foot proportions have been chosen similar to the human foot. Anyway, it is possible to optimize the arc proportions, which represent for the ankle the arm of the contact-force at heel-strike and toe-off, according to stability or efficiency criteria.

5. Actuators control

5.1 The spring-damper actuator

The twelve actuated degrees of freedom are actuated by an elastic actuator. The actuator is composed by a servo motor (a big servo with 24 kg cm torque), a torsional spring and a damper, as illustrated in Fig. 14. The resulting assembly is small, lightweight and simple. Using a spring between the motor and the joint let us have a precise force feedback simply measuring the deflection of the spring. The resulting actuator has a good shock tolerance; fundamental in walking, as impacts occur at every step. In addition, we can exploit the natural dynamic of the link storing energy in the spring.
Similar actuators, with a DC motor and a spring, have been successfully used in biped robotics by (Pratt et al. , 1995) (Takanishi et al, 1997)

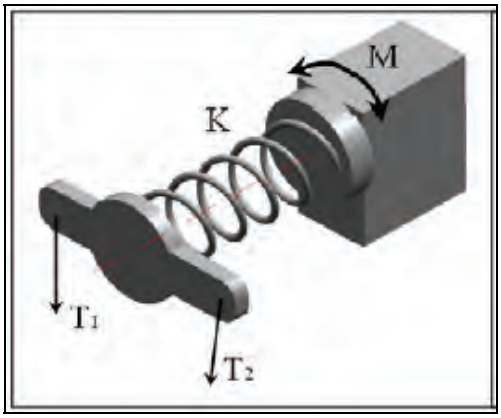

Fig. 14. The schema of the elastic actuator.

The choice of the servos and the materials was made basically on cheap and off-the-shelf components. The main characteristic of this actuator is that the joint stiffness is not infinite,

as it is in servo motors, and it can be changed in real time despite the constant stiffness of the spring. This has been achieved through a right choice of spring-damper characteristics and thanks to an intuitive control algorithm.
Let define the joint stiffness kg as:

$$kg = Me/\varepsilon \tag{4}$$

where Me is the external load and ε is the position error.
A first prototype of our actuator was composed by two motors and two springs, working as agonist and antagonist muscles in humans. This let us to vary the joint stiffness even when no external load is acting, pre-tensioning the joint. With only one motor and one spring, the initial stiffness of the joint is fixed by the spring constant, since the motor needs some time to tension the spring and counteract the external torque. Also, in this conditions, the presence of the damper in parallel to the spring permits to avoid high initial errors due to rapidly varying loads.

The damping factor can be chosen constant, at its critical value ξ=1.

$$wn = \sqrt{(kg/I)} \text{ and } d = 2\,\xi wnI \tag{5}$$

or can be varied during motion, in order to save motor torque and make the system faster. In the following paragraph we present the first option.

5.2 The control algorithm for a fixed damping factor

The spring-damper actuator can be used in a torque control loop: the high-level controller assigns the torque to be delivered and, measuring the spring deflection, the low-level regulator makes the actuator perform the task.
A way to assign joint torques is the Virtual Model Control (Pratt et al. 2001). In this approach, the controller sets the actuator torques using the simulation results of a virtual mechanical component. In such a manner the robot can benefits of the component behavior without having it really.
In other classical approaches (Kwek et al, 2003) the calculation of the joint torques is based instead on the dynamic model of the robot, usually complicated and imprecise. Indeed the biped robot can be formalized with a multi-input-multi-output (MIMO) non linear system, that sometime presents also time variant dynamical behavior. In these conditions a classical PID (Proportional Integral Derivative) controller is not suitable and more complex control strategies are needed. On the other hand, if we apply only a simple position controller we lack the control of the joint stiffness.
To solve these issues we developed a simple algorithm that can control the joint stiffness and position providing the worth torque without complex calculations. While a high-level controller assigns the trajectories, as in classical position control, the elastic low-level regulator varies the joint stiffness in real time and makes a smooth motion.
In addition, we developed a more articulated algorithm with acceleration and velocity feedback; it provides an estimation of the external torque acting on the link, and modifies

the joint stiffness accordingly. These algorithms are described in detail in the next two subsections.

5.2.1 The controller using position feedback

The basic control algorithm is simple and very closed to a classical model of the Equilibrium Point hypothesis. It takes in input the reference position ϕr and the joint stiffness kg and gives in output the motor position α_0 The only state information needed is the actual joint position, that must be measured and feed-backed to the regulator. We may remind that the difference between the actual position and the motor one is covered by the spring deflection. The control law is expressed by equation 6:

$$\alpha_0 = (kg/k)\,(\phi r - \phi) + \phi \tag{6}$$

where k represent the spring stiffness, ϕr and ϕ the target and actual angular position respectively. The result is that a virtual spring with kg stiffness is acting between the reference angle and the actual position. For kg =k, $\alpha 0 = \phi r$, as the spring and joint stiffness coincide. If kg<k the motor rotation will be lower than the reference, as the spring stiffness is higher than the one required for the joint. Dually, if kg>k the motor has to rotate more to generate higher torques. Thus, the choice of kg and k can depend on the motor characteristics: kg>k attenuates the effects of a motor position error, while kg<k is suited when the motor limit is the speed.

For the other input, the reference position, to avoid high initial acceleration ϕr should be defined with second order functions with suited time constants. The finite joint stiffness betokens the presence of an error and one may define the time when the desired position must be reached, accordingly with the joint stiffness.

If stiffness is very high, the error will be small, and the actual trajectory very close to the assigned one; this means that in presence of a step in ϕr high acceleration peaks can be generated.

If the joint stiffness is small, one may expect relevant differences between the reference and actual trajectories, as the inertia and the damping oppose to fast movements. The static error ε depends anyway on the external load T_{ext} as in equation 7:

$$\varepsilon = T_{ext}/kg \tag{7}$$

Equation 7 represents also a way to determine the joint stiffness, deciding the maximum error tolerance and estimating the external maximum load. Note that kg can be changed in real time, according to the precision needed in critical phases of the motion. To define the reference trajectory we used a step function filtered by a second order filter defined by a suited time constant T. In this way we can characterize the reference pattern with a single parameter. For simplicity the damping factor is set to a constant value that keep the system at the critical damping, as in equation 5

We simulated the control of a simple 1-dof pendulum to confirm the theoretical approach. In the simulation, gravity and external loads were included. Also friction was included to test the robustness of the algorithm.

We set the system parameters as: m=1.2 kg; l=0.3 m; Ig=7.35*10-2 kgm2; k=6 Nm/rad; kg=10 Nm/rad (where l is the distance between the center of mass and the joint axis).
Fig. 15 (a) shows the joint angles and motor positions of the system for a commanded movement from 0 to 0.3 rad at 0.1 sec, and from 0.3 rad to -0.3 rad at 1.2 sec with a constant time T=0.08 s. Here, only gravity is acting, but tests were made including variable external disturbances, which could mimic the inertia load of other moving links. With "static angle", we denote the position the joint would have if the link inertia was zero and the damper was not present. The chosen stiffness is quite weak, and the error is about 0.1 rad only due to gravity. Looking at the motor position, we can notice that it is always opposite to the angle respect to the reference since the spring stiffness is chosen lower than the joint stiffness. In this way the motor has to rotate more, but the system is less sensitive to motor position error. At about 1.4 sec., the motor rotation changes velocity due to servo maximum torque limit. In the simulation also servo speed limitation was included.
About the resulting rotational acceleration, we can notice in Fig. 14 (b) only two peaks, acceleration and deceleration, with no oscillation. This pattern, typical of damped systems, is useful when it is needed to exploit the natural dynamics of multi-link systems. For instance, when starting a step, the acceleration of the thigh can be used to bend the knee, as in passive dynamic walkers (McGeer, 1990)(Collins et al, 2001) or, before foot-fall, the deceleration of the swing motion can be exploited to straight the leg, as in passive lower-limb prosthesis.

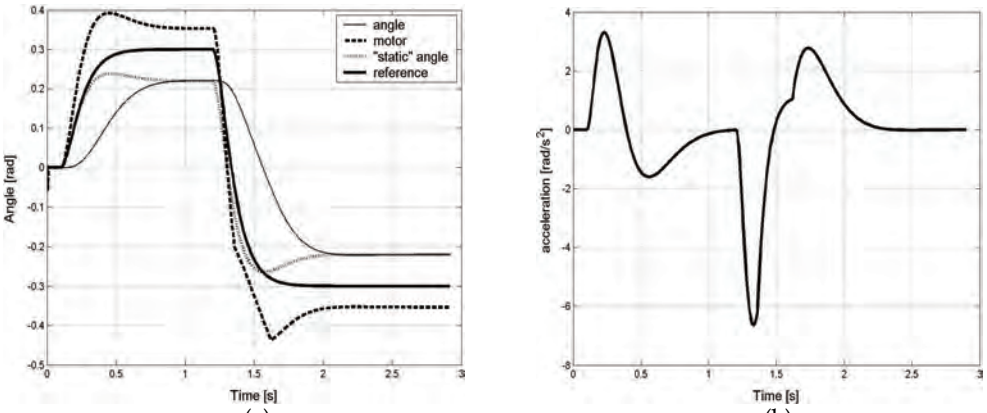

(a) (b)

Fig. 15. (a) The link rotation and the motor position referred to the commanded angle. The actual angle approaches the reference accordingly to the stiffness and external load ("static" angle). (b) The acceleration pattern presents two peaks, characteristic of damped systems. The change at about t=1.5 s is due to the limit on servo maximum torque.

To figure out the influence of rapidly external loads, we studied a positioning task under step-varying external torque. Here the stiffness was set high, since a keep-position task was to be performed: k=10 Nm/rad; kg=50 Nm/rad. Figure 16 shows the result of the system under the action of an external load composed by a sinusoidal and constant action; at 0.1s there is a positive step; at 1s a negative one.

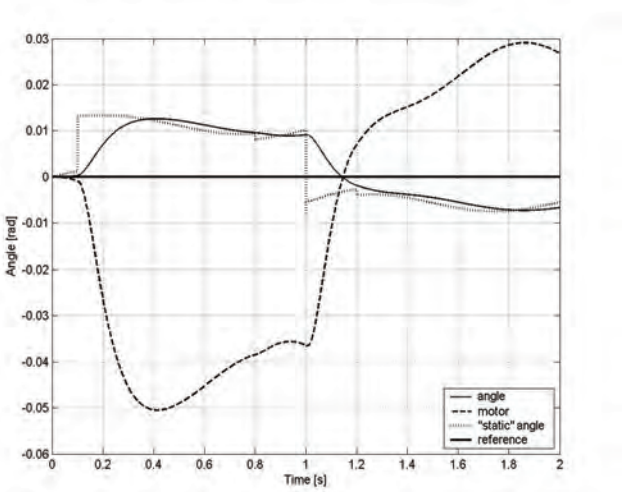

Fig. 16. The system behavior under rapidly-varying external torques. These can be seen in the "static angle" changing accordingly to the sinusoidal and step components of the load.

Using this simple control law, we do not need to solve any inverse dynamic problem, but just decide the joint stiffness, using for example equation (7), and define the suited reference pattern. Different is the case when, given a reference trajectory, we want to follow it controlling the motor torque; in this case, the external load plays a very important role, while, with the elastic control, we just need a rough estimate of it when the joint stiffness is fixed.
The following subsection describes a more complete algorithm that can automatically adapt joint stiffness to the external load, given system inertia, or its average value for a multi-link system.

5.2.2 Force estimation through acceleration feedback

In trajectory planning, not only the position is constrained, but also the velocity and acceleration must respect some limitations. This is especially important when we want to exploit the natural dynamic of the multi-body system; the acceleration of the thigh can be used to bend the knee when starting the step (McGeer, 1990) or to straight it before the foot-fall, as in passive leg prosthesis. Also velocity and acceleration limitations are needed where inertial loads, due to the movement of one part, can interfere with the motion of the rest of the robot; this is particularly relevant in bipedal walking.
To consider acceleration constrains, we included in our controller a sort of impedance control. By this term, we refer to the fact that the algorithm tracks the delivered torque and studies the resulting acceleration, creating a function relating these two quantities. In this way, we can create a simple dynamic model of a multi-body system without solving any inverse dynamic problem. The model can also get a good estimate of the external load acting on the joint, including gravity and the interaction force with other links.
This can be obtained using, in the control loop, the equations (8):

$$T^{i-1}{}_{ext} = -k \cdot (\alpha_0{}^{i-1} - \varphi^{i-1}) + I \cdot \ddot{\varphi}^{i-1} + d \cdot \dot{\varphi}^{i-1} \tag{8}$$

where d is the damping factor (as in equation 5), α_0 is obtained from equation (6), I is the inertia and k an elastic constant. We can assume that between the instants i-1 and i of the control loop the external load remains constant, so $T^{i-1}{}_{ext} = T^{i}{}_{ext.}$
Given the values of k, d, I, the position of the motor a_0 and the estimation of $T_{ext.,}$ the acceleration can be estimated from equation (9):

$$Ai = (k \cdot (\alpha_0{}^{i} - \varphi^{i}) + T^{i-1}{}_{ext} - d \cdot \dot{\varphi}^{i}) / I \tag{9}$$

In this way we implement a kind of impedance control: if the acceleration (system output) in the next step is different from the foreseen one, given the calculated α_0 (system input), system infers that a different load is acting (system model has changed) and thus the motor position α_0 is corrected accordingly. In some way this is also how we sample the properties of objects in real word. For instance, to check whether a bin is empty or not we lift it, and according to the resulting motion we estimate the mass. In a positioning task, we make this sample-evaluation-correction every instant.
The simulations on a single joint, with parameters: m=1.2 kg; l=0.3 m; Ig =7.3510^{-2} kg m^2, k=10 Nm/rad; kg=50 Nm/rad, are discussed, evaluating position, acceleration, and external load. In Fig. 17 we illustrate the results on the angle, with and without limiting the motor torque and using as external load only the gravitational one.

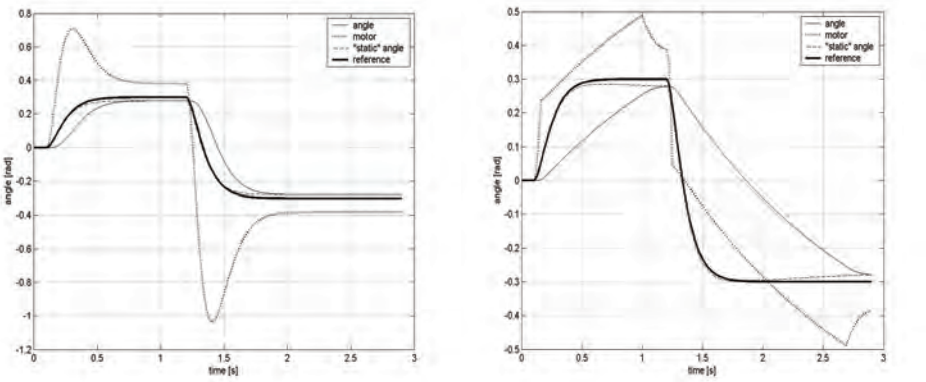

Fig.17. the angles with and without torque limitation

We can notice in Fig 18 the effect of limiting motor torque on the acceleration pattern. The characteristic is similar to the human electro-myographic activity, composed by there phases: acceleration-pause-deceleration (Kiriazov, 1991) (Gotlieb et al, 1989) and suitable for exploiting the natural dynamic of the links, i.e. in leg swinging as pointed out before. We can also notice that the system perform a pretty good estimation of the external load acting on the link.

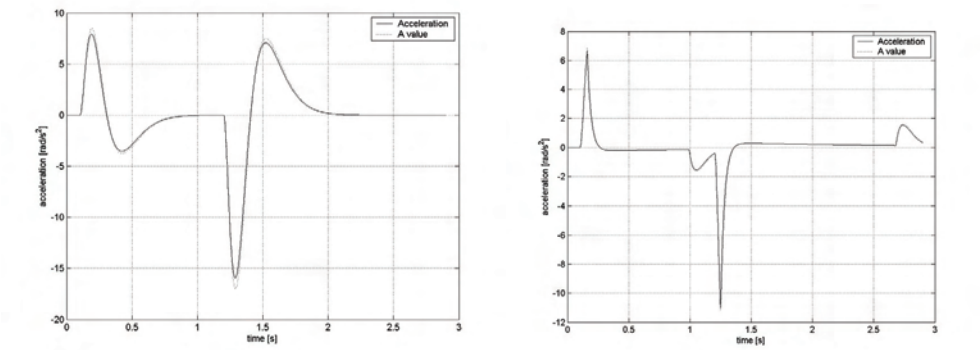

Fig. 18. the acceleration with and without motor torque limitation is considered.

If we impose a joint stiffness too high for the load applied, or if the reference angle changes too quickly, the controller decreases joint stiffness during the motion to prevent too high accelerations. This is performed using the calculated acceleration for the incoming iteration (equation 9) If, with the imposed stiffness, the acceleration A^i is too high, the low-level controller modifies kg (given by the high-level algorithm), to respect acceleration limits. In this way the real value of the acceleration is kept below its maximum value, despite wrong high-level commands.

Setting joint stiffness can be done with equation 7, or with a trial-and-error procedure. For example, a learning algorithm could be used to kg and the time constant of the reference trajectory. The choice of these two parameters as inputs for the low-level regulator is relevant since they can greatly influence the joint behavior, without hampering the final positioning.

The only information the controller needs about the system is its inertia. In multi-link systems it can be approximated with a constant average value computed on all the links, or it can be calculated during the motion. In any case, the controller seems to be quite robust respect to inertia uncertainties, showing no relevant changes even for errors of about 30% (see figure 19). The difference in inertia load is considered by the controller as an additional external torque. The damping, equation (5) can be rewritten as(10):

$$d = 2\xi\sqrt{kgI_i} \tag{10}$$

This means that the damping factor is proportional to the square root of inertia errors: while a too high inertia makes the system over-damped, an underestimation can let the system oscillate. Anyway, the error in the inertia must be very high (such as 50%) to see noticeable effects on the damping.

In the external torque estimation (Fig. 19) we can notice the effect of wrong inertia input in the controller: for instance, if the real inertia value is higher, the controller acts as an additional external load is braking rotation during positive accelerations, as the real inertia is higher than what expected. In this way, the system is "automatically compensated".

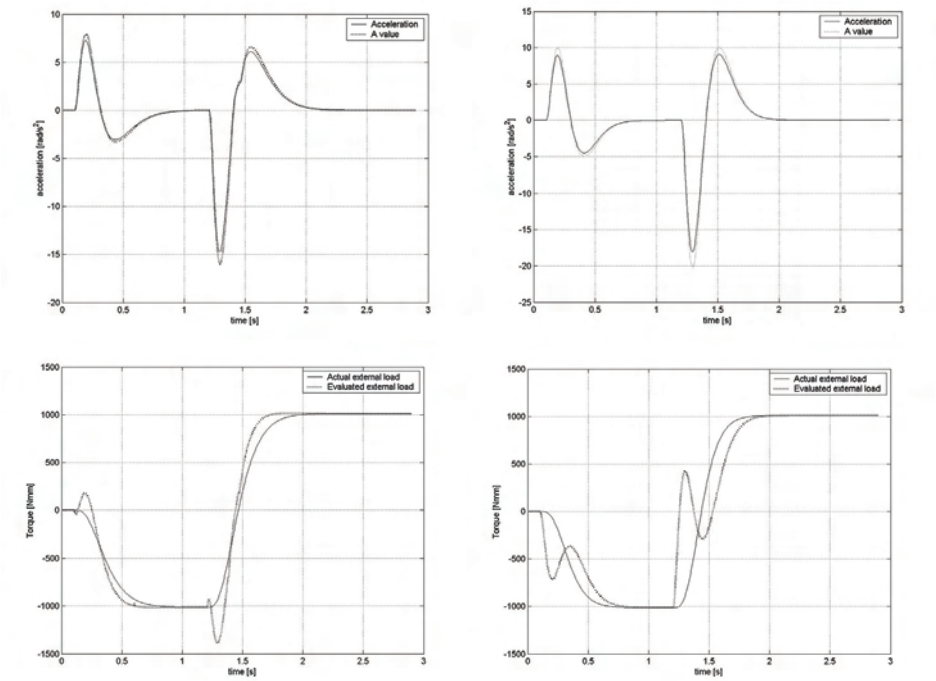

Fig. 19. Overestimated, on the left, and underestimated inertia on the right. Top row shows acceleration, bottom row torque.

From Fig 19 we may observe that an error of 30% in inertia does not compromise the positioning. If the computed inertia is lower than the real one, for example when the system is accelerating, the algorithm interprets the too small acceleration as an external load. When the computed inertia is higher than the real one, the system is over-accelerated, and a virtual additional positive torque is considered acting.

5.3 Results on LARP

The spring-reactive control has been implemented in a computer simulation on the simple robot model of Fig. 2, and after on the real prototype. In the first test, the robot had to preserve the equilibrium despite external disturbances. To run this test we implemented also a simplified physical prototype of LARP, with two dof in the ankle (pitch and roll) and one in the hip (yaw) for each leg.

Figure 20 shows the external disturbances applied on the robot. The joint stiffness is set according to equation 7, where ε is the maximum error and T_{ext} is the corresponding gravitational load. The value of inertia is calculated focusing on the resulting damping more than on the real value, that should be computed along the closed kinematic chain formed by the biped. Thus, for the ankle, we figure out the inertia of the robot considering the two feet coincident. Given this inertia value, we evaluate the needed total damping factor d. As in the feet two dampers in parallel are present, we split the inertia so that the sum of the two

dampers equals the total damping needed. Regarding the hip, we proceed in the same way, neglecting the leg beneath the joint for computing inertia.

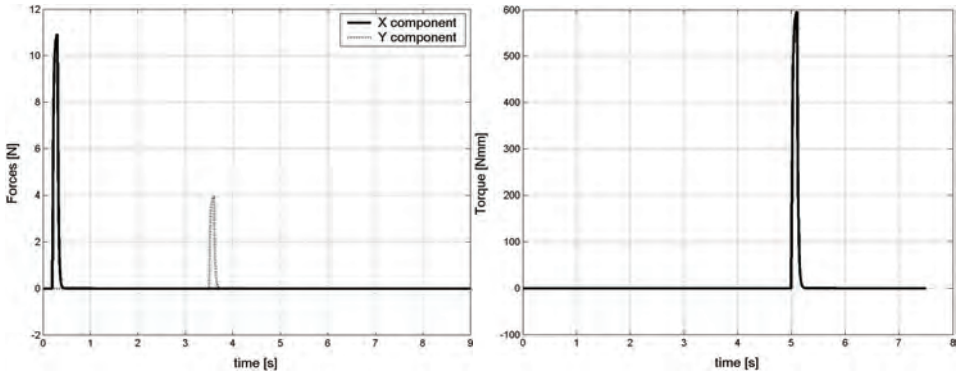

Fig. 20. The external disturbances applied to the robot, forces and torque.}

The results are shown in figure 21, where we can notice that a position error appears when the disturbance is applied, as the actual angle differs from the reference position zero. The dotted line shows the motor rotation, that counteracts the disturbance and brings the joint back to the reference. In this way the robot is able to "react" to external loads, admitting a positioning error in order to preserve the whole balance.

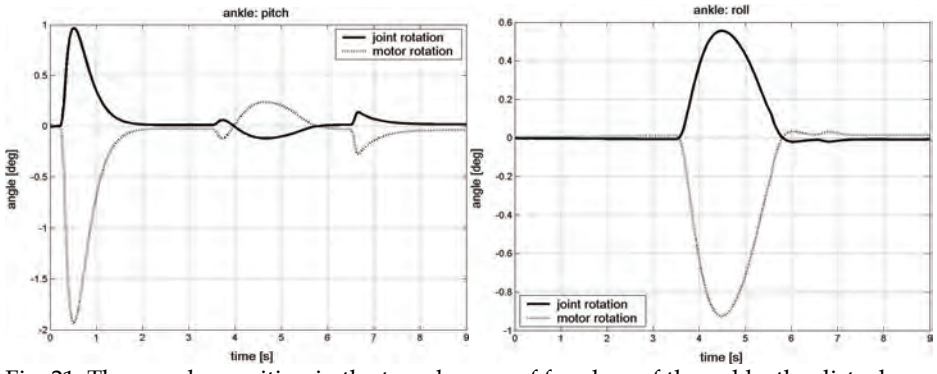

Fig. 21. The angular position in the two degrees of freedom of the ankle: the disturbances are adsorbed and the robot returns in its initial position.

6. Simulation of a static gait and energy consumption

In this section we present some results we have obtained using the direct/inverse kinematic model of our biped. We do not enter in details of this models, but we prefer concentrate our attention on energetic considerations. We also want to stress here that simulations are very important for complex projects like our robot, and this is more important if the hardware is not yet completed. The movement of the biped robot was performed using elastic actuators

and a controller based on the Equilibrium Point Hypothesis (Scarfogliero et al, (a and b), 2004), as illustrated in the previous Section.
Using the inverse kinematic solution, we can set a reference trajectory for the foot and calculate the relative joints positions. Each gait is characterized by

- the step length and height,
- the minimum height that the pelvis is allowed to reach during the motion, and
- the maximum lateral movement admissible (oscillations in frontal plane).

During all the motion the robot assumes only stable configurations, this means that if we arrest the movement the robot will keep the balance. A sufficient condition for the static stability for the robot is that the projection of its center of mass falls inside the convex area that cover the contact surface of the two feet. In our simulation the static stability is always guarantee by a software module that adjusts the pelvis position when the stability condition is not verified.
To evaluate the energy required to complete a step we made the following assumptions and approximations:

- Each robot link is modelled by a mass located in its center of mass.
- The center of mass for the entire robot is calculated by a weighted average of each link's center of masses.
- The robot moves very slowly, therefore inertia forces are neglected.
- We do not consider friction forces present in the joints.
- We consider that kinetic energy during the falling phase (the lifted foot approaches the ground) is completely lost during the movement.

The energy to lift each single link was therefore calculated with equation 11, where m is the mass of the link-i, g the gravity constant and Δh_i the excursion along the z-axis for the center of mass of link-i.

$$W_i = m_i \, g \, \Delta h_i \tag{11}$$

Clearly we have approximated the real energy required for the movement, but our aim is to distinguish between efficient and non efficient gaits.
In the simulation shown in Fig. 22, we settled the step length at 0.5m, the minimum height for the pelvis at 0.68m and the maximum lateral excursion at 0.09m (oscillation in frontal plane).

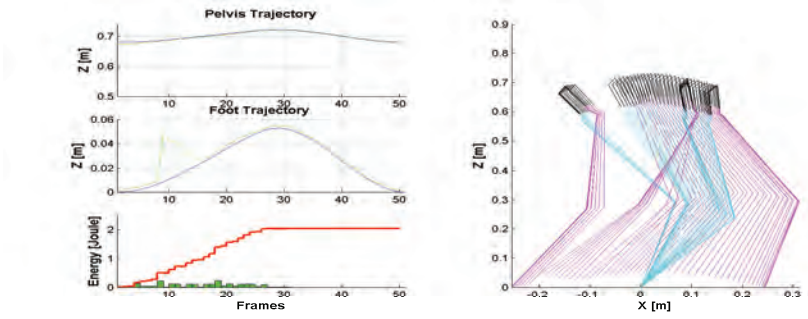

Fig. 22. Energy consumption with minimum height for pelvis at 0.68m}

The first two graphs in the left part of fig. 21 represent the Z coordinates for the pelvis and the foot during the motion (in blue the reference trajectory, in green the real trajectory performed by the robot). From the third graph in the left side we see that the total energy consumed to perform the gait is about 2 joules. It is possible to note that at the eighth frame the real foot trajectory deviates significantly from the reference, as a result of the stability algorithm that tries to maintain the balance. Finally the graph in the right site shows a stick model for the robot in the lateral plane and gives us an overview of the all gait's phases.
In the simulation shown in Fig. 23, we set the minimum height allowed for the pelvis at 0.55m. This means that the robot, when following the reference trajectory, is allowed to lower more its *cm*. In this case the reference trajectory for the foot is well followed, nevertheless the energy required for this gait is increased to about 6 joules. This is due to the fact that the links of the robot have a greater excursion along the z axis.

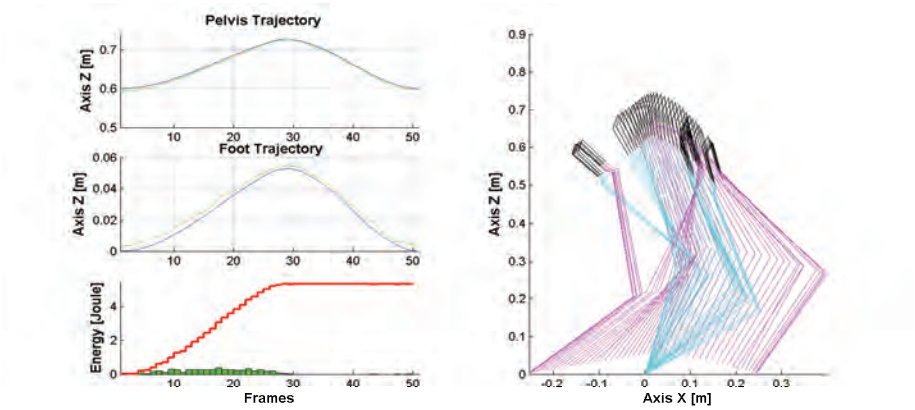

Fig. 23. Energy consumption with minimum height for pelvis at 0.60m

These preliminary results confirm that the position of the *cm* of the robot has a great impact on energy consumption. If the *cm* is maintained low the stability algorithm does not interfere with the trajectory following for the foot in static condition. Nevertheless these kind of postures require more energy, while limiting the vertical movement of the pelvis can save energy during the gait. We can also assert that the knee joint covers a very important role during the gait, indeed without this degree of freedom it is difficult move down the robot's *cm* and therefore stabilize the posture.
The strategy to decrease the height of the *cm* is advantageous to control the robot stability if we are in static conditions (at low acceleration and velocities the inertia forces can be neglected), nevertheless with this kind of posture the robot is not able to perform fast walking, and also the energy required for the movement is high. The human walking, on the contrary, can be assumed as dynamical; indeed in each instant the body is not in a stable position. Furthermore the pelvis is maintained high and as fixed as possible to reduce the energy required for the movement, as indicated in our results.
To be energetically efficient our robot should be tested also in dynamical conditions, to take advantage of the knee and foot design that were thought to store the inertia and impact forces.

7. Simulation of the robot's dynamic behaviour

To better account for the many elements that act in the real situations we developed a MSC Adams model of the robot, to compute in real time the forces through a Simulink application, whose general architecture is illustrated in Fig. 24. Three are the main modules.

- The force generation module is a closet loop system that generates the correcting forces to apply to the links, proportional to the difference between the target position and the sensed position.
- The ZMP controller is a closed loop controller that generates a correction force, proportional to the difference between the ideal and the real position of the ZMP.
- The 3D simulator animates the ADAMS model, as illustrated in Fig. 24.

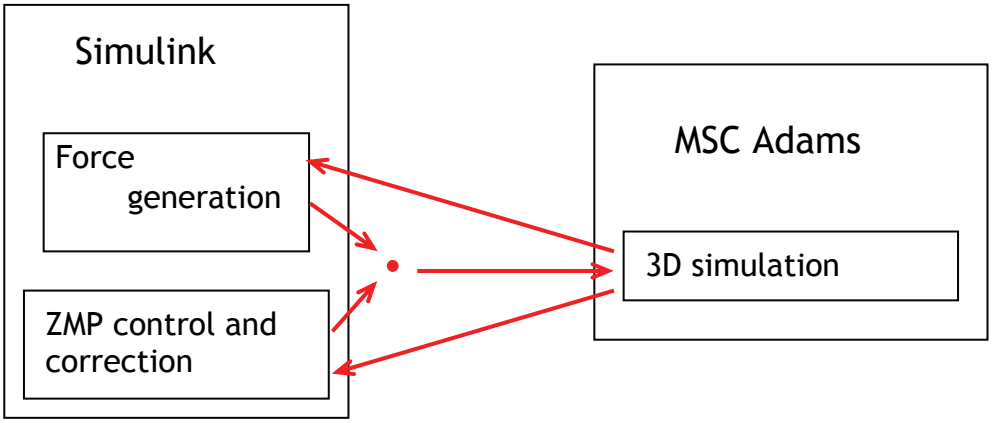

Fig. 24. The architecture of the LARP simulator.

To simulate a step using our dynamic simulator we start from recorded joint positions, that are used to generated both the static and dynamic robot gaits. Those positions are called *frames* and are obtained from measures from human beings.
The gate is composed of 3 phases, each represented by different frames:

- start – contains 11 frames and moves the robot from the initial idle configuration to the move phase;
- move – contains 44 frames; the robot makes 2 steps for each move phase, and returns to the initial configuration. We can repeat this phase as many times as we want;
- stop – contains 11 frames and is the reverse of the start phase; the robot goes from the move phase to the initial idle position.

Starting from the joint positions, and using the Newton-Eulero equations, in theory we can compute from equation 12 forces and moments that act on the center of mass of each link and send the so obtained values, with a given frequency, to the actuators to obtain the trajectory.

$$F_i = m\dot{v}c_i$$
$$N_i = {}^{Ci}I\dot{\omega}_i + {}^{Ci}I\omega_i \tag{12}$$

To obtain dynamic stability we use the Zero Moment Point (ZMP) criterion. Using the data from the sensors on the links we compute the x and y coordinates of the Zero Moment Point according to equation 13:

$$x_{ZMP} = \frac{\sum_{i=1}^{n} m_i(\ddot{z}_i + g)x_i - \sum_{i=1}^{n} m_i\ddot{x}_i z_i - \sum_{i=1}^{n} T_{yi}}{\sum_{i=1}^{n} m_i(\ddot{z}_i + g)}$$
$$y_{ZMP} = \frac{\sum_{i=1}^{n} m_i(\ddot{z}_i + g)y_i - \sum_{i=1}^{n} m_i\ddot{y}_i z_i - \sum_{i=1}^{n} T_{xi}}{\sum_{i=1}^{n} m_i(\ddot{z}_i + g)} \tag{13}$$

where:

i indicates the link number
T is the torque applied by the motor
m is the mass
g is the gravity acceleration
(x,y,z) is the center of mass of the link
$(\ddot{x}, \ddot{y}, \ddot{z})$ is the link acceleration

We developed an algorithm for the dynamic stability, where the real ZMP is compared with the ideal ZMP. Since the most instable phase is the one of single support, we correct the errors in this phase. The parameters of the algorithm are:

- *nframes*, number of frames in the single support phase;
- *lfoot* and *wfoot*, length and width of the foot;

For each value of the independent variable *actualframe* we obtain the ideal x and y coordinates of the ZMP, x_{ID} and y_{ID}, using the equation 14:

$$x_{ID}(actualframe) = \frac{lfoot}{nframes} * actualframe$$
$$y_{ID}(actualframe) = \frac{3}{4}lfoot - \left(\left(actualframee - \frac{nframes}{2} \right)^2 * \frac{\frac{wfoot}{2}}{\left(\frac{nframes}{2} \right)^2} \right) \tag{14}$$

The coordinates are relative to a reference system in the foot, with origin in the intersection point between the back and the inner sides of the foot, with the x-axis in the direction of the foot point and y-axis that points to the external side of the foot.
Suppose the ideal trajectory of the ZMP point linearly moves along the x-axis and quadratically moves along the y-axis from $\frac{1}{4}wfoot$ to $\frac{3}{4}wfoot$ in $\frac{1}{2}nframes$, *and* simmetrically, from $\frac{3}{4}wfoot$ to $\frac{1}{4}wfoot$ in $\frac{1}{2}nframes$.
The obtained trajectory is parabolic, as in humans, and is illustrated in Figure25.

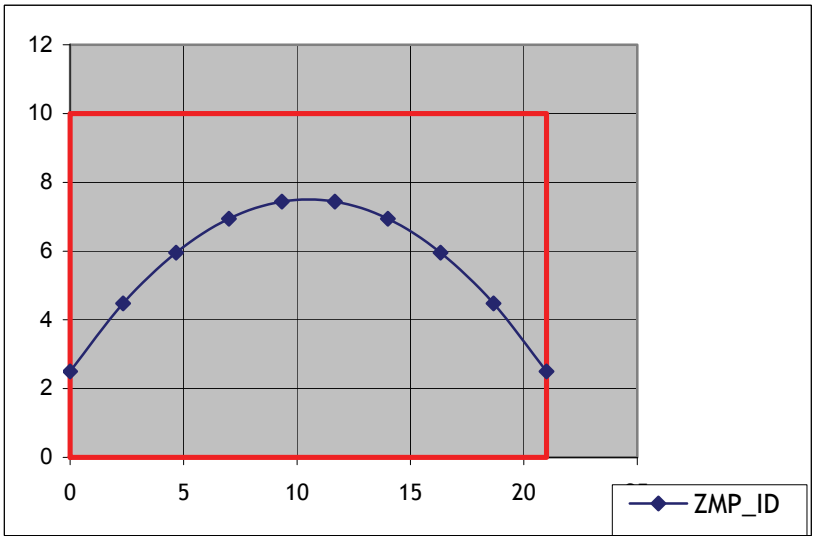

Fig. 25. Trajectory of the ideal ZMP for the left foot of LARP (in red the area of the foot)

Comparing x_{ID}, y_{ID} and x_{ZMP}, y_{ZMP} we compute the errors with equation 15:

$$\begin{aligned} \varepsilon_x(actualframe) &= x_{ID}(actualframe) - x_{ZMP}(actualframe) \\ \varepsilon_y(actualframe) &= y_{ID}(actualframe) - y_{ZMP}(actualframe) \end{aligned} \quad (15)$$

We compute the corrective force F_{CORR} to apply to the hip joints as in equation 16:

$$F_{CORR}(actualframe) = \alpha * \varepsilon(actualframe) + \beta * (\varepsilon(actualframe-1) - \varepsilon(actualframe)) \quad (16)$$

with α and β constants. The correction is proportional to the error and to its trend. The actuators in the hip apply the total force F_{TOT} (equation 17):

$$F_{TOT}(actualframe+1) = F_T(actualframe+1) + F_{CORR}(actualframe) \quad (17)$$

where F_T is the offline computer force necessary to obtain the wanted trajectories.
The controller schema in Simulink is illustrated in Appendix A.

7.1 Results in simulation

We have experimented on LARP two situations, namely maintaining the standing position, and walking.

7.1.1 Maintaining the standing position

To keep the robot in standing position we assign zero values to the angles of movement, and detach the subsystem devoted to the stability control of walking. In the following figures 26, 27, and 28 we see the positions (in meters) and the torques (in Nm) applied to the left hip, left knee, and left ankle respectively, all around the y axis.

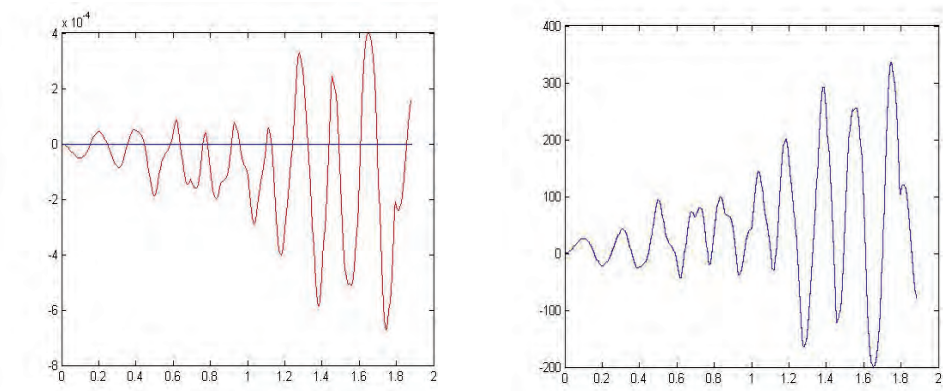

Fig. 26 Sensed position and moment applied to the left hip around the y axis.

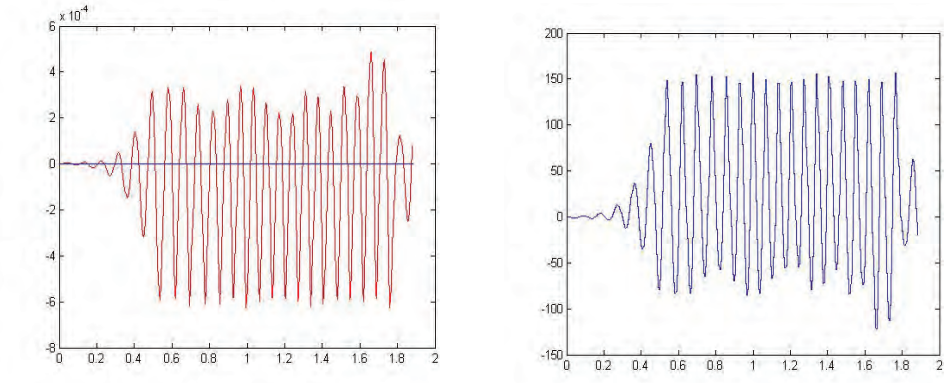

Fig. 27. Sensed position and moment applied to the left knee around the y axis.

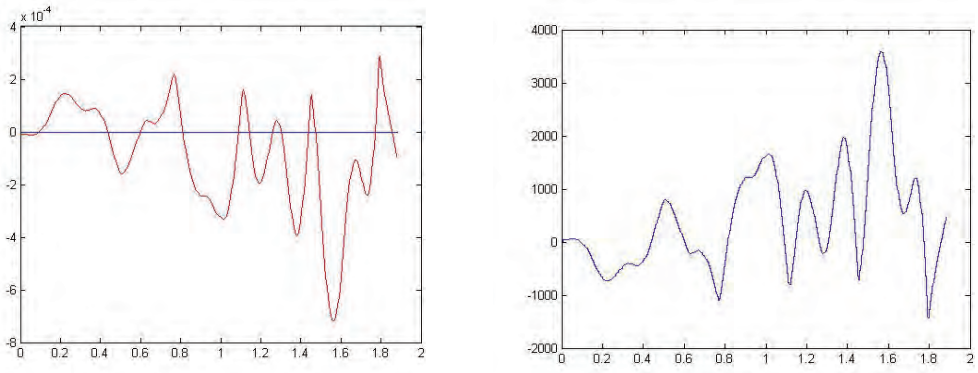

Fig. 28. Sensed position and moment applied to the left ankle around the y axis.

The three joints have a similar behavior; after few oscillation it stabilizes. Observe that the maximum error is really small, about 0,5 mm.

7.1.2 Walking

In simulating the dynamic walking new problems emerged.
First, since walking for bipeds is a really dynamic situation, more and different parameters are involved.
The most important problem in LARP is the position of the center of mass. Until now LARP has no torso, so the maximum height for the center of mass is the pelvis. The inertia acting on the pelvis cannot be compensated, as in humans, from the arm movements, so it generates oscillations that in some cases cannot be compensated.
Another problem is the foot. The real foot has a flat surface, but in simulation a flat surface requires to consider too many points, and is impractical. To speed up the simulation we model the flat surface as eight small spheres, with only eight point contacts. This solution reduces the friction and the robot can slip. For those reason the simulation of the gait should be stopped after a few steps. The addition of the torso will be done for future simulations.

8. Conclusions

LARP is a project about developing a biped robot in parallel with the study of human walking. Some images of the mechanical construction are in Appendix 2.
Today several humanoids robots are able to walk and perform human-like movements. Anyhow, the structure of such robots significantly differs from the human's one. This causes the robots to be energetically inefficient, as they are unable to exploit the natural dynamics of the links, and very poorly adaptable to unstructured terrains.
Studying the human knee and foot we found several advantages in adopting human-oriented design for these parts. In particular, a compliant knee was developed, having two circular contact surfaces and five tendons. This articulation is highly efficient and permits to increase the foot clearance during the swing phase. Regarding the foot, two passive joints were introduced to mimic the high mobility of the human foot. To ensure stability both at

heel-strike and toe-off we used two planar surfaces connected to the arc of the foot by two passive degrees of freedom.
Further work has to be done for the complete design of a human-like robot, starting from a new design of hip and ankle articulation. In this case we should investigate the role of the third dof in the human ankle (torsion of the foot along the leg axis), which is omitted in most of the modern humanoid robots. Also, it remains to fully test our model in dynamical condition, in order to find the more efficient and efficacious gait.
The similarity between the behavior of our robot and of human walking can be exploited to promote a further research comparing the biped behavior with human theories assumptions.

9. References

R. Alexander, *The Human Machine*. Columbia University Press. New York, 1992.

F. A. Asatryan, D.G., "Functional tuning of the nervous system with control of movement or maintenance of a steady posture - mechanographic analysis of the work of the joint or execution of postural task," *Biofizika*, vol. 10, pp. 837–846, 1965.

D.G. Asatryan, A.G. Feldman.(a), "Functional tuning of the nervous system with control of movement or maintenance of a steady posture - ii controllable parameters of the muscle," *Biofizika*, vol. 11, pp. 498–508, 1966.

D.G. Asatryan, A.G. Feldman (b), "Functional tuning of the nervous system with control o movement or maintenance of a steady posture - iii mechanographic analysis of the work of the joint or execution of a postural task, *Biofizika*, vol. 11, pp. 667–675, 1966.

S. Collins, M. Wisse, and A. Ruina, "A three dimensional passivedynami walking robot with two legs and knees," *The Internationa Journal of Robotics Research*, vol. 20, no. 7, pp. 607–615, 2001.

J. Doneland, R. Kram, and D. A. Kuo, "Simultaneous positive and negative external mechanical work in human walking," *Journal o Biomechanics*, vol. 35, pp. 117–124, 2002.

G. Fallis, "Walking toy," *U.S. Patent No.376588*, 1888.

M. Garcia, A. Chatterje, A. Ruina, M.J. Coleman, "The simplest walking model Stability, complexity and scaling," *ASME Journal of Biomechanica Engineering Vol. 120 p.281-288*, vol. 120, pp. 281–288, 1998.

G. Gottlieb, Q. Song, D. Hong, G. Almeida, D. Corcos., "Co-ordinating movement a two joints: a principle of linear covariance," *Neurophysiology*, vol. 75 no. 5, pp. 1760–1764, 1996.

G. L. Gottlieb, D.M. Corcos, G.C. Agarwal., "Strategies for the control of single mechanical degree of freedom voluntary movements," *Behavioral an Brain Sciences*, vol. 12, no. 2, pp. 189–210, 1989.

S. Hashimoto at al., "Humanoid robots in waseda university hadaly 2 an wabian," *Autonomous Robots*, vol. 12, pp. 25–38, 2002.

K. Hirai, M. Hirose, Y. Haikawa, T. Takenaka., "The development of honda humanoid robot," *IEEE International Conference on Robotics and Automation* pp. 1321–1326, 1998.

A. Jeanneau, J. Herder, T. Lalibert´e, and C. Gosselin, "A compliant rolling contact joint and its application in a 3-dof planar parallel mechanism with kinematic analysis," *In Proc. DETC 2004 Salt Lake City, Utah*, 2004.

R. Ker, M. Bennett, S. Bibby, R. Kerster, and R. M. Alexander, "The spring in the arc of the human foot," *Nature*, vol. 325, pp. 147–149 1987.

P. Kiriazov., "Humanoid robots: How to achieve human-like motion," *Journal of Biomechanics*, no. 24, pp. 21–35, 1991.

B. Koopman, F. van der Helm, and P. Veltink, *Human motion control*. University of Twente, Enschede; University of Technology, Delft, 2001.

A. D. Kuo., "Stabilization of lateral motion in passive dynamic walking, *The International Journal of Robotics Research*, vol. 18, no. 9, pp 917–930, 1999.

A. D. Kuo, "Energetics of actively powered locomotion using the simples walking model," *ASME Journal of Biomechanical Engineering* vol. 124, pp. 281–288, 1998.

L. C. Kwek, E. K. Wong, C. K. Loo, M. V. C. Rao, "Application of active force control and iterative learning in a 5-link biped robot," *Journal of Intelligent and Robotic Systems*, vol. 37, no. 2, pp. 143–162, 2003.

M.L. Latash., G.L. Gottlieb, "An equilibrium-point model for fast single-join movement. similarity of single-joint isometric and isotonic descendin commands," *Journal of Motor Behavior*, vol. 23, pp. 163–191, 1991.

H.-O. Lim, S. A. Setiawan, and A. Takanishi, "Position-based impedance control of a biped humanoid robot," *Advanced Robotics* vol. 18, no. 4, pp. 415–435, 2004.

G. Maloiy, N. Heglund, L. Prager, G. Cavagna, and C. Taylor "Energetic costs of carrying loads: have african women discovere an economic way?" *Nature*, vol. 319, pp. 668–669, 1986.

T. McGeer, (a) "Passive dynamic walking," *The International Journal o Robotics Research*, vol. 9, no. 2, pp. 62–82, 1990.

T. McGeer, (b)"Passive walking with knees," *IEEE International Conferenc on Robotics and Automation*, vol. 2, pp. 1640–1645, 1990.

J. McIntyre and E. Bizzi, "Servo hypotheses for biological control o movement," *Journal of Motor Behavior*, vol. 25, no. 3, pp. 193–202 1993.

J. Pratt, C. Chew, A. Torres, P. Dilworth, and G. Pratt, "Virtual model control: An intuitive approach for bipedal locomotion," *The International Journal of Robotics Research*, vol. 20, no. 2, pp. 129 143, 2001.

G.A. Pratt , M.M. Williamson, "Series elastic actuators," *IEEE International Conferences on Intelligent Robots and Systems*, no. 1, pp. 399–406 1995.

P. Sardain, M. Rostami, E. Thomas, and G. Bessonnet, "Biped robots Correlations between technological design and dynamic behaviour, *Control Engineering Practice*, vol. 7, pp. 401–411, 1999.

J. Saunders, V. Inman, and H. Eberhart, "The major determinants in normal and pathological gait," *Journal of Bone and Joint Surgery*, vol 35-A, pp. 543–558, 1953.

U. Scarfogliero, M. Folgheraiter, G. Gini, (a) "Advanced steps in biped robotics: Innovative design and intuitive control through springdampe actuator," *In Proc. IEEE Humanoids 2004, Los Angeles, USA* 2004.

U. Scarfogliero, M. Folgheraiter, G. Gini (b) "Larp: Biped robotic conceived as human modelling," *In Proc. Neurobotics KI 2004, Ulm Germany*, 2004.

R. Sallaouti, O. Stasse, S. Kajita, K. Yokoi, A. Kheddar, "Faster and smoother walking of Humanoid HRP-2 with passive toe joints", Proc IEEE IROS 2006,.

C. Vaughan, "Are joint torques the holy grail of human gait analysis? *Human Movement Science*, vol. 15, pp. 423–443, 1996.

T. A. Yamaguchi J., "Design of biped walking robot having antagonistic driven joint using nonlinear spring mechanism," *IROS 97*, pp 251–259, 1997.
M. Wisse and J. Frankenhuyzen, "Design and construction of mike; a 2d autonomous biped based on passive dynamic walking." *Delft University of technology*, 2002.
M. Wisse, A. L. Schwab, R. Q. vd. Linde., "A 3d passive dynamic biped wit yaw and roll compensation," *Robotica*, no. 19, pp. 275–284, 2001.

APPENDIX 1 - The Simulink schema of the controller for the dynamic stability of the robot

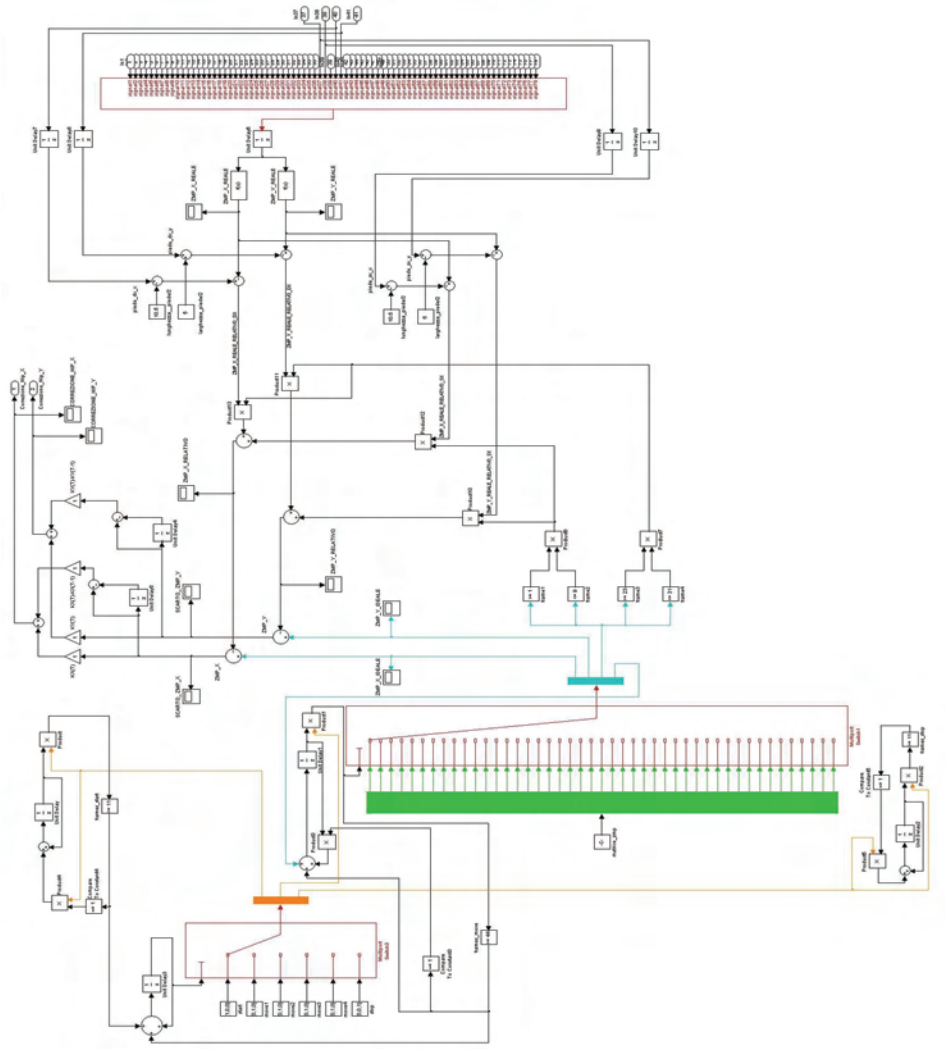

APPENDIX 2 – Images of LARP

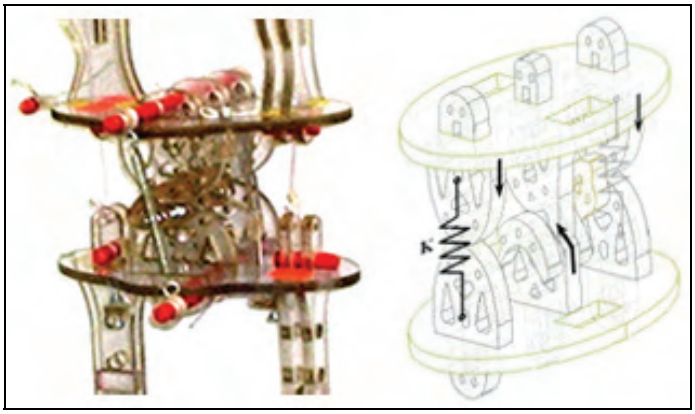

The knee

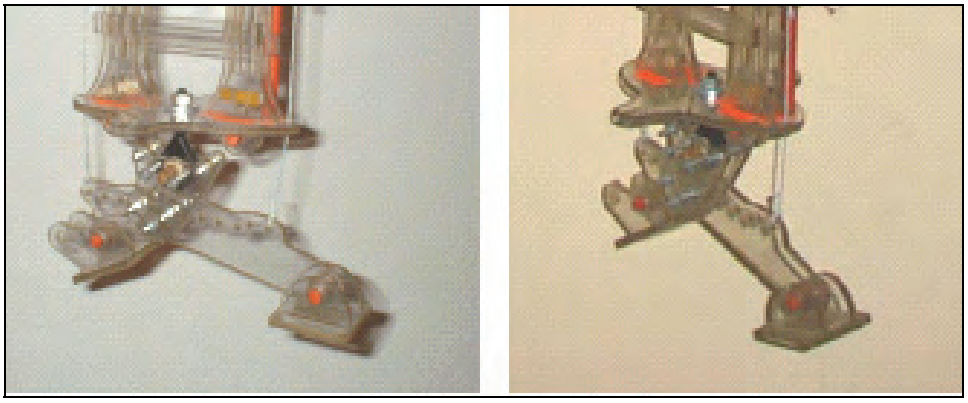

The ankle

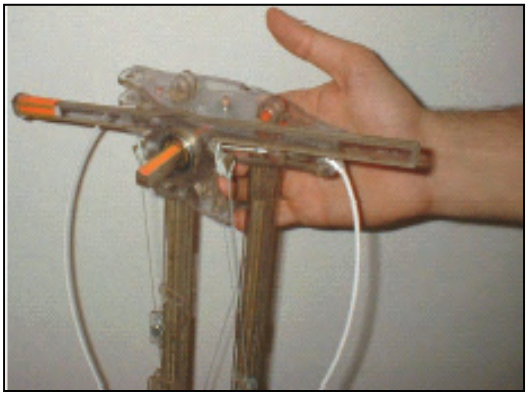

The hip

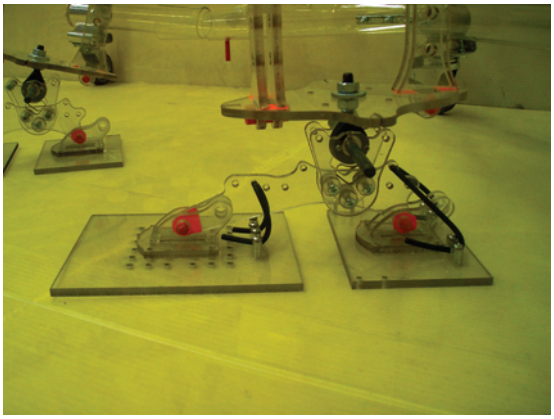

The foot

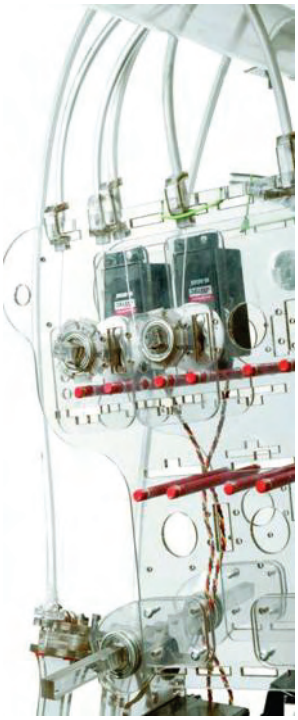

The actuators area over the hip